

Nonlinear Attitude Control for a Picosatellite

J. R. Córdova Alarcón¹, E. Vicente Vivas¹ and H. Rodríguez Cortés²

¹ Instituto de Ingeniería, UNAM

Ciudad Universitaria, México, D. F., México.

² Centro de Investigación y Estudios Avanzados-IPN,

Departamento de Ingeniería Eléctrica,

Av. IPN 2508, San Pedro Zacatenco, México, D.F., México.

Resumen This paper addresses the attitude stabilization problem for a picosatellite. The proposed solution consists of a nonlinear controller based on a combination of two nonlinear control design techniques, backstepping and exact tracking error dynamics passive output feedback. Numerical simulations show the performance of the proposed controller.

1. Introduction

During the last two decades there has been a gradual tendency to rearrange Earth-orbiting architectures from the single large satellite architecture to constellations of a number of small satellites. Constellations of small satellites promise better mission flexibility and success by distributing the tasks and by reducing the possibility of a catastrophic failure. If one small satellite of the constellation fails, others can continue operating until a replacement is launched.

As a consequence, a fast growing small satellite industry has enabled increasingly capable and cost-effective space missions by embracing reduced requirements and integrating commercial technology. This growing small satellite interest has also spread throughout the academic research and has resulted in nanosatellites (< 10kg) and picosatellites (< 1 kg) with an emphasis on decreasing the size through application of advanced technologies while trading off capability. In this framework, the California Polytechnic State University (Cal Poly) at San Luis Obispo together with the Space Systems Development Laboratory (SSDL) at Stanford University developed the CubeSat program whose aim is to provide a standard low-cost platform to design a class of picosatellites, called CubeSats [1].

The work reported in this paper is part of a study of possible actuators configurations and control methods and for the CubeSat type picosatellite developed by the Engineering Institute from the National Autonomous University of Mexico and the Research and Advanced Studies Centre of the National Polytechnic Institute. The main mission of this picosatellite is to take pictures of the Earth so that an accurate attitude control system becomes absolutely necessary.

The attitude control problem for a fully actuated spacecraft has received considerable attention by the control design community. In particular, in [9] a

large family of globally stable control laws is obtained by using the globally non-singular unit quaternion attitude representation in an energy inspired Lyapunov function. Using non minimal attitude representations in [8] passivity properties of the spacecraft kinematics and dynamics are presented. Based on these passivity properties, linear asymptotic stabilizing controllers and control laws without angular velocity measurements are also introduced. In [7] an adaptive control scheme for attitude control is derived by using a linear parameterization of the spacecraft dynamics; global convergence of the tracking error to zero is shown using passivity arguments. In [10] the attitude control of a rigid spacecraft with a cluster of N variable speed control moment gyroscopes is considered from the perspective of passivity. Finally, in [4] the attitude stabilization is solved via a structure variable controller using a minimal attitude representation and in [3] the attitude control problem is solved using the backstepping control design technique using a quaternion representation of attitude.

In this paper the attitude stabilization problem for a picosatellite is addressed and solved. The proposed solution consists of a nonlinear controller based on a combination of two nonlinear control design techniques, backstepping and exact tracking error dynamics passive output feedback. The exact tracking error dynamics passive output feedback control design technique, introduced in [5], has been applied successfully to solve control problem in the power electronics field and lately has been applied to solve control problems in mobile robotics [6]. Numerical simulations show the performance of the proposed controller.

The rest of the paper is organized as follows: Section 2 defines the different reference frames used in the paper and introduces the picosatellite kinematics and dynamics. Section 3 is devoted to control design, and numerical simulation results are presented in Section 4. Conclusions and perspectives of future work are stated in Section 5.

2. Picosatellite attitude dynamics

The following coordinate systems are used to define the picosatellite attitude dynamics, see Figure 1.

Earth centered inertial coordinate system. This coordinate system is labeled by \mathcal{S}^I and has its origin located in the center of the Earth. The x_i axis is oriented to the vernal equinox, the z_i axis points toward the North pole and the axis y_i completes a right handed orthogonal frame.

Orbital coordinate system. The origin of this coordinate system, labeled as \mathcal{S}^O , is in the satellite center of mass. The z_o axis points to the Earth's centre, the x_o axis points in the direction of the orbital velocity vector and the y_o axis is normal to the satellite orbit plane. Assuming a near circular orbit, the orbital coordinate system rotates relative to the Earth centered inertial coordinate system with an angular velocity given approximately by [2]

$$\Omega_o \approx \sqrt{\frac{gr_e^2}{r_c^3}}$$

where g is the gravity constant at sea level, r_e is the Earth's radius and r_c is the distance from the origin of the orbital coordinate system to the center of the Earth.

Satellite fixed coordinate system. This coordinate system, labeled as \mathcal{S}^B , has its origin in the satellite center of mass; it is usual to assume that these axes coincide with the satellite's principal inertia axes. In our particular application we consider that the picosatellite weight distribution is such that the z_b axis is perpendicular to the lens of a high resolution camera. The other axis is selected in order to complete a right handed orthogonal triad. The satellite fixed coordinate system will match with the orbital coordinate system when the satellite attitude is zero degrees in roll, pitch and yaw angles.

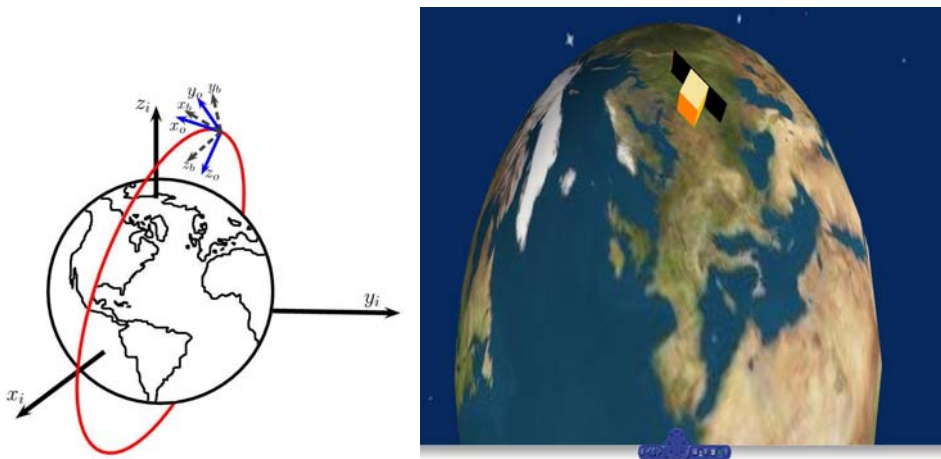


Figure 1. (Right) Coordinate systems. (Left) Virtual reality environment.

Picosatellite's kinematics. Vectors related to the picosatellite's kinematics can be expressed in terms of any of the previously described coordinate systems and the relationship between those coordinate systems is done by rotation matrices, denoted by R , members of the special orthogonal group

$$SO(3) = \left\{ R \mid R \in \mathbb{R}^{3 \times 3}, R^T R = I, \det R = 1 \right\}$$

The rotation matrix can be expressed in terms of the four Euler parameters as follows

$$R = I - 2\eta S(\epsilon) + 2S^2(\epsilon) \quad (1)$$

where

$$\eta = \cos\left(\frac{\beta}{2}\right) \in \mathbb{R}, \quad \epsilon = \lambda \sin\left(\frac{\beta}{2}\right) \in \mathbb{R}^3$$

with θ the rotation about the arbitrary unit vector λ . The coordinate transformation of a vector r from coordinate system \mathcal{S}^A to coordinate system \mathcal{S}^B is given by $r^b = R_a^b r^a$. Finally, the time derivative of a rotation matrix can be expressed as follows

$$\dot{R}_a^b = R_a^b S(\Omega_{ab}) \quad (2)$$

where Ω_{ab} is the angular velocity of coordinate system \mathcal{S}^B relative to coordinate system \mathcal{S}^A and $S(\cdot)$ is the cross product operator given by

$$x \times y = S(x)y = \begin{bmatrix} 0 & -x_3 & x_2 \\ x_3 & 0 & -x_1 \\ -x_2 & x_1 & 0 \end{bmatrix} y$$

The four Euler parameters define the unit quaternion $q = [\eta \ \epsilon^\top]^\top$, with

$$\eta^2 + \epsilon^\top \epsilon = 1 \quad (3)$$

The picosatellite's kinematics equations expressed in terms of the unit quaternion can be obtained from (1) and (2) as

$$\begin{aligned} \dot{\eta} &= -\frac{1}{2} \epsilon^\top \Omega_{ob} \\ \dot{\epsilon} &= \frac{1}{2} [\eta I + S(\epsilon)] \Omega_{ob} \end{aligned} \quad (4)$$

where Ω_{ob} is the angular rate of the picosatellite fixed coordinate system \mathcal{S}^B relative to orbital coordinate system \mathcal{S}^O .

Picosatellite's dynamics. The picosatellite attitude dynamics, found from Newton's second law, is described by the following differential equations

$$J \dot{\Omega}_{ib} - S(J \Omega_{ib}) \Omega_{ib} = \tau \quad (5)$$

where $\Omega_{ib} \in \mathbb{R}^3$ is the vector of angular rates of the picosatellite fixed coordinate system \mathcal{S}^B relative to the Earth centered inertial coordinate system \mathcal{S}^I , $J = \text{diag}[J_{xx}, J_{yy}, J_{zz}] \in \mathbb{R}^{3 \times 3}$ is the picosatellite inertia matrix and τ is the vector of external torques due to the inertia wheels.

The relationship between the angular velocity of the picosatellite fixed coordinate system relative to the orbital coordinate system and the angular velocity of the picosatellite fixed coordinate system relative to the Earth centered inertial coordinate system is defined as

$$\Omega_{ob} = R_o^b \Omega_{io} + \Omega_{ib} \quad (6)$$

where $\Omega_{io} = [0 \ \Omega_o \ 0]^\top$, $R_o^b = I - 2\eta S(\epsilon) + 2S^2(\epsilon)$.

3. Control design

Attitude error. Given a desired picosatellite attitude

$$q_d = [\eta_d \ \epsilon_d^\top]^\top$$

the attitude error quaternion is given by

$$\tilde{q} = q_d \otimes q = \begin{bmatrix} \eta_d \eta + \epsilon_d^\top \epsilon \\ \eta_d \epsilon - \eta \epsilon_d - S(\epsilon_d) \epsilon \end{bmatrix} = \begin{bmatrix} \tilde{\eta} \\ \tilde{\epsilon} \end{bmatrix} \quad (7)$$

where \otimes is the quaternion product operator. Note that the picosatellite kinematics expressed in terms of the quaternion error is described by the following equations

$$\begin{aligned} \dot{\tilde{\eta}} &= -\frac{1}{2} \tilde{\epsilon}^\top \Omega_{ob} \\ \dot{\tilde{\epsilon}} &= \frac{1}{2} [\tilde{\eta} I + S(\tilde{\epsilon})] \Omega_{ob} \end{aligned} \quad (8)$$

Backstepping. Here we design the first part of the proposed nonlinear controller inspired on the backstepping methodology. For, let us define

$$y = \Omega_{ob} - \Omega_{ob_d} \quad (9)$$

where

$$\Omega_{ob_d} = \pm \frac{\Delta \tilde{\epsilon}}{1 + \tilde{\epsilon}^\top \tilde{\epsilon}} \quad (10)$$

with $\Delta = \text{diag}\{\delta, \delta, \delta\}$ a positive definite matrix. Replacing (9) into (8) one has

$$\begin{aligned} \dot{\tilde{\eta}} &= -\frac{1}{2} \tilde{\epsilon}^\top (\Omega_{ob_d} + y) \\ \dot{\tilde{\epsilon}} &= \frac{1}{2} [\tilde{\eta} I + S(\tilde{\epsilon})] (\Omega_{ob_d} + y) \end{aligned} \quad (11)$$

Consider now the following Lyapunov function

$$V_1 = (\tilde{\eta} \pm 1)^2 + \tilde{\epsilon}^\top \tilde{\epsilon} \quad (12)$$

whose time derivative along the dynamics (11) is given by

$$\dot{V}_1 = -\frac{\Delta \tilde{\epsilon}^\top \tilde{\epsilon}}{1 + \tilde{\epsilon}^\top \tilde{\epsilon}} \pm \tilde{\epsilon}^\top y$$

thus, by driving y to zero we have that $\tilde{\epsilon} = 0$ and by LaSalle theorem, considering (3), we conclude that $\tilde{\eta} = \mp 1$. Note now that equation (9) can be written in terms of Ω_{ib} as follows

$$y = (R_o^b \Omega_{io} + \Omega_{ib}) - \Omega_{ob_d} \quad (13)$$

defining

$$\Omega_{ib_d} = \Omega_{ob_d} - R_o^b \Omega_{io} \quad (14)$$

we have

$$y = \Omega_{ib} - \Omega_{ib_d} \quad (15)$$

Now, we design a controller to drive y to zero using the exact tracking error dynamics passive output feedback control design technique.

Exact tracking error dynamics passive output feedback. Consider the following general model of physical systems,

$$\begin{aligned} \mathcal{A} \dot{x} &= \mathcal{J}(x, u) x - \mathcal{R}(x, u) x + \mathcal{B}(x) u + \mathcal{E}(t) \\ y &= \mathcal{B}^\top x \end{aligned} \quad (16)$$

where x is an n dimensional vector, \mathcal{A} is a constant symmetric, positive definite matrix, $\mathcal{J}(x, u)$ is a skew symmetric matrix, $\mathcal{R}(x, u)$ is a symmetric positive definite matrix and $\mathcal{E}(t)$ is a n -dimensional smooth vector function of t or sometimes, a constant vector. The input matrix $\mathcal{B}(x)$ is a $n \times m$ matrix and, hence the output vector y is an m dimensional vector. Moreover, we assume that

$$\begin{aligned}\mathcal{J}(x, u) &= \mathcal{J}_0 + \sum_{j=1}^m \mathcal{J}_j^u u_j + \sum_{k=1}^n \mathcal{J}_k^x x_k, \quad \mathcal{B}(x) = \mathcal{B}_0 + \sum_{k=1}^n \mathcal{B}_k x_k \\ \mathcal{R}(x, u) &= \mathcal{R}_0 + \sum_{j=1}^m \mathcal{R}_j^u u_j + \sum_{k=1}^n \mathcal{R}_k^x x_k\end{aligned}\quad (17)$$

Consider now that

- A1 Given a feasible smooth bounded reference trajectory $x^*(t) \in R^n$, there exists a smooth open loop control input $u^*(t) \in R^m$, such that for all trajectories starting at $x(t_0) = x^*(t_0)$, the tracking error $e(t) = x(t) - x^*(t)$ is identically zero for all $t \geq t_0$.
- A2 For any constant positive definite symmetric matrix K the following relation is uniformly satisfied

$$\mathcal{D}^*(x, u, t) = \mathcal{R}^*(x, u, t) + \mathcal{B}^*(x, t)K\mathcal{B}^*(x, t)^\top > 0$$

Theorem 1. Consider the system (16)-(17) in closed loop with the controller

$$u = u^*(t) - K\mathcal{B}^*(x, t)e \quad (18)$$

Then, under assumptions A1 and A2, the tracking error $e(t)$ is globally asymptotically stabilized to zero.

Demostración. Let us define $e_u = u - u^*(t)$ and the following

$$\begin{aligned}\mathcal{M}^*(t) &= [(\mathcal{J}_1^x - \mathcal{R}_1^x) x^*(t) \cdots (\mathcal{J}_n^x - \mathcal{R}_n^x) x^*(t)], \quad \mathcal{L}^*(t) = [B_1 x^*(t) \cdots B_n x^*(t)] \\ \mathcal{Q}^*(t) &= [(\mathcal{J}_1^u - \mathcal{R}_1^u) x^*(t) \cdots (\mathcal{J}_m^u - \mathcal{R}_m^u) x^*(t)]\end{aligned}\quad (19)$$

Straightforward computations show that the error dynamics reads as

$$\mathcal{A}\dot{e} = [\mathcal{J}^*(x, u, t) - \mathcal{R}^*(x, u, t)]e + \mathcal{B}^*(x, t)e_u, \quad y_e = \mathcal{B}^*(x, t)^\top e \quad (20)$$

where

$$\begin{aligned}\mathcal{J}^*(x, u, t) &= \mathcal{J}(x, u) + \frac{1}{2} [\mathcal{P}^*(t) - \mathcal{P}^*(t)^\top], \quad \mathcal{B}^*(x, t) = \mathcal{B}(x) + \mathcal{Q}^*(t) \\ \mathcal{R}^*(x, u, t) &= \mathcal{R}(x, u) - \frac{1}{2} [\mathcal{P}^*(t) + \mathcal{P}^*(t)^\top]\end{aligned}\quad (21)$$

with $\mathcal{P}^*(t) = \mathcal{M}^*(t) + \mathcal{L}^*(t)$. We refer to (20) as the exact open loop error dynamics. Take now the following Lyapunov function candidate

$$V = \frac{1}{2} e^\top \mathcal{A} e \quad (22)$$

whose time derivative along the closed-loop dynamics (20)-(18) is given by

$$\dot{V} = -e^\top [\mathcal{R}^*(x, u, t) + \mathcal{B}^*(x, t)K\mathcal{B}^*(x, t)^\top] e$$

By A2 the proof is completed.

Note that the picosatellite dynamics can be written in the form of the general model (16) with

$$\mathcal{A} = J, \mathcal{J}(x) = S(J\Omega_{ib}), \mathcal{R}(x, u) = 0, \mathcal{B} = I, \mathcal{E}(t) = 0 \quad (23)$$

so that it is possible to obtain the tracking error dynamics. Note that in this case (15) plays the role of e and

$$\tilde{\tau} = \tau - \tau_d$$

with

$$\tau_d = J\dot{\Omega}_{ib_d} - S(J\Omega_{ib_d})\Omega_{ib}$$

plays the role of e_u in Theorem 1. Straight forward computations show that

$$\mathcal{L}^*(T) = \mathcal{Q}^*(t) = 0, \mathcal{B}^* = I$$

and

$$\mathcal{M}^*(t) = \begin{bmatrix} 0 & J_{yy}\Omega_{ib_{d3}} & -J_{zz}\Omega_{ib_{d2}} \\ -J_{xx}\Omega_{ib_{d3}} & 0 & J_{zz}\Omega_{ib_1} \\ J_{xx}\Omega_{ib_{d2}} & -J_{yy}\Omega_{ib_{d1}} & 0 \end{bmatrix}$$

as a result, we have

$$\mathcal{J}^*(x, t) = \begin{bmatrix} 0 & \frac{1}{2}A_j & -\frac{1}{2}B_j \\ -\frac{1}{2}A_j & 0 & \frac{1}{2}C_j \\ \frac{1}{2}B_j & -\frac{1}{2}C_j & 0 \end{bmatrix} \quad (24)$$

where $A_j = (J_{xx} + J_{yy})\Omega_{ib_{d3}} - 2J_{zz}\Omega_{ib_3}$, $B_j = (J_{xx} + J_{zz})\Omega_{ib_{d2}} - 2J_{yy}\Omega_{ib_2}$ and $C_j = (J_{yy} + J_{zz})\Omega_{ib_{d1}} - 2J_{xx}\Omega_{ib_1}$. Moreover,

$$\mathcal{R}^*(t) = \begin{bmatrix} 0 & \frac{1}{2}A_r\Omega_{ib_{d3}} & -\frac{1}{2}B_r\Omega_{ib_{d2}} \\ \frac{1}{2}A_r\Omega_{ib_{d3}} & 0 & \frac{1}{2}C_r\Omega_{ib_{d1}} \\ -\frac{1}{2}B_r\Omega_{ib_{d2}} & \frac{1}{2}C_r\Omega_{ib_{d1}} & 0 \end{bmatrix} \quad (25)$$

with $A_r = J_{xx} - J_{yy}$, $B_r = J_{xx} - J_{zz}$, and $C_r = J_{yy} - J_{zz}$. Thus, the tracking error dynamics is described by the following equations

$$\mathcal{A}\dot{y} = [\mathcal{J}^*(x, t) - \mathcal{R}^*(t)]y + \tilde{\tau} \quad (26)$$

Now we verify that assumption A2 is satisfied. Note that by selecting $K = \text{diag}\{k, k, k\}$ we have

$$\mathcal{D}^*(t) = \begin{bmatrix} k & \frac{1}{2}A_r\Omega_{ib_{d3}} & -\frac{1}{2}B_r\Omega_{ib_{d2}} \\ \frac{1}{2}A_r\Omega_{ib_{d3}} & k & \frac{1}{2}C_r\Omega_{ib_{d1}} \\ -\frac{1}{2}B_r\Omega_{ib_{d2}} & \frac{1}{2}C_r\Omega_{ib_{d1}} & k \end{bmatrix}$$

It is easy to verify that $\mathcal{D}^*(t)$ is a positive definite matrix provided the constant k is selected in such a way that the following inequalities are satisfied

$$k > 0, k > \frac{1}{2}A_r\sigma_1, k > \frac{\frac{1}{6}(108c + 12\sqrt{12b^3 + 81c^2})^{\frac{2}{3}} - 2b}{(108c + 12\sqrt{12b^3 + 81c^2})^{\frac{1}{3}}} \quad (27)$$

where $c = \frac{1}{4}A_r B_r C_r \sigma_1^3$, $b = -\frac{1}{4}(A_r^2 + B_r^2 + C_r^2)\sigma_1^2$ and we have used the fact that

$$\Omega_{ib_d} = -\frac{\Delta\tilde{\epsilon}}{1 + \tilde{\epsilon}^\top \tilde{\epsilon}} - R_o^b \Omega_{io} \quad (28)$$

is a bounded signal, that is,

$$\|\Omega_{ib_d}\| \leq \frac{\delta}{2} + |\Omega_{io}| = \sigma_1 \quad (29)$$

as

$$\left\| \frac{\Delta\tilde{\epsilon}}{1 + \tilde{\epsilon}^\top \tilde{\epsilon}} \right\| \leq \frac{\delta}{2}, \quad \|R_o^b\| \leq 1 \quad (30)$$

Finally, we have

Proposition 1. *Consider the differential equations (4)-(5) that describe the kinematics and dynamics of a picosatellite in closed loop with the controller*

$$\tau = \mp\tilde{\epsilon} \mp K\Delta\frac{\tilde{\epsilon}}{1 + \tilde{\epsilon}^\top \tilde{\epsilon}} - K(\Omega_{ib} + R_o^b \Omega_{io}) + \tau_d \quad (31)$$

Then for any k that satisfies (27) and any $\delta > 0$ the equilibrium point

$$[\eta^*, \epsilon^*, \Omega_{ib}^*]^\top = [\eta_d, \epsilon_d, R_o^b(\eta_d, \epsilon_d)\Omega_{io}]^\top$$

is globally asymptotically stable.

Demostración. Note that in terms of the tracking errors $\tilde{\eta}$, $\tilde{\epsilon}$ and y the picosatellite behavior is described by equations (11) and (26). Moreover, the control law (31) in terms of tracking errors reads as

$$\tilde{\tau} = \mp\tilde{\epsilon} - Ky$$

Consider now the Lyapunov function

$$V = (\tilde{\eta} \pm 1)^2 + \tilde{\epsilon}^\top \tilde{\epsilon} + \frac{1}{2}y^\top \mathcal{A}y$$

it is straight forward to verify that its time derivative along the trajectories of the system (11) and (26) in closed loop with (31) is given by

$$\dot{V} = -\frac{\Delta\tilde{\epsilon}^\top \tilde{\epsilon}}{1 + \tilde{\epsilon}^\top \tilde{\epsilon}} - y^\top \mathcal{D}^*(t)y$$

Due to the fact that the time varying terms in $\mathcal{D}^*(t)$ are uniformly bounded this matrix is positive definite uniformly. Then, by LaSalle Theorem we have that

$$\lim_{t \rightarrow \infty} \tilde{\epsilon} = 0, \quad \lim_{t \rightarrow \infty} y = 0$$

finally, as the quaternion error represents a rotation it follows that $\tilde{\eta}^2 + \tilde{\epsilon}^\top \tilde{\epsilon} = 1$. As a consequence $\tilde{\eta} = \pm 1$. This concludes the proof.

Remark 1. It is possible to verify that

$$\|\pm\tilde{\epsilon}^\top y + \tau_d\| \leq \kappa_1 + \kappa_2 \|y\|$$

for some positive constants κ_1 and κ_2 . Therefore, in the numerical simulations of the next Section we consider the control law given by $\tau = -Ky$.

4. Simulations results

Numerical simulations were carried out to evaluate the performance of the proposed controller. The picosatellite parameters consider the weight distribution of a CAD model of the picosatellite developed by the Engineering Institute from the National Autonomous University of Mexico and the Research and Advanced Studies Centre of the National Polytechnic Institute. From the CAD model we obtain the inertia parameters as $J_{xx} = 0,001905\text{Kg}\cdot\text{m}^2$, $J_{yy} = 0,002905\text{Kg}\cdot\text{m}^2$ and $J_{zz} = 0,00248\text{Kg}\cdot\text{m}^2$. We consider $r_e = 6378\text{Km}$, $r = 7378\text{Km}$ and $g = 9,81\text{m/s}$. This gives $\Omega_o = 0,0009968\text{rad/s}$ that corresponds to an orbit period of approximately 6300 s. We have also implemented the picosatellite dynamics in a virtual reality environment in order to verify that all rotations involved are satisfactory, see Figure 1. Figure 2 shows the attitude error and the

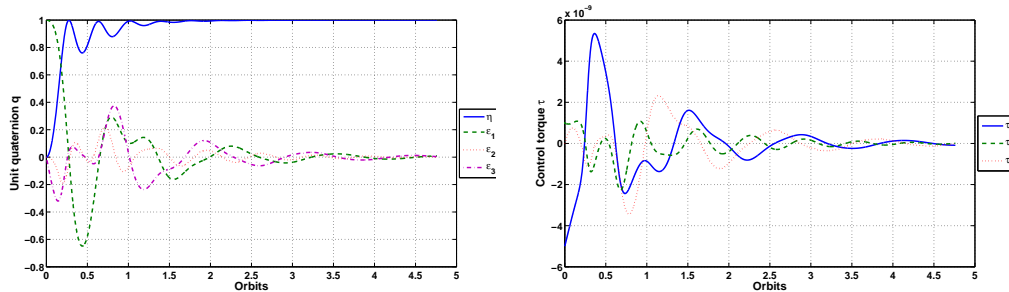


Figure 2. (Right) Attitude error for $q_d = [1 \ 0 \ 0 \ 0]^\top$. (Left) Relative angular rate Ω_{ob} .

control torque for $q_d = [1 \ 0 \ 0 \ 0]^\top$ while Figure 3 shows the attitude error and control torque for $q_d = [-1 \ 0 \ 0 \ 0]^\top$. As it can be observed the tracking errors converge to the desired value with bounded control inputs. In both simulations we consider $q(0) = [0 \ 1 \ 0 \ 0]^\top$, $\Omega_{ob}(0) = [0 \ 0 \ 0]^\top$ and the controller gains $\delta = 0,000001$, $k = 0,01$.

5. Conclusions

We have presented a nonlinear controller that solves the attitude stabilization problem of a picosatellite. The proposed controller is based on a combination of two successful control design methodologies: backstepping and exact tracking error dynamics passive output feedback. The controller performance was evaluated through numerical simulations and a virtual reality implementation.

Some issues are left open in this paper. First, we do not provide a formal proof showing global asymptotic stability of the desired equilibrium point for

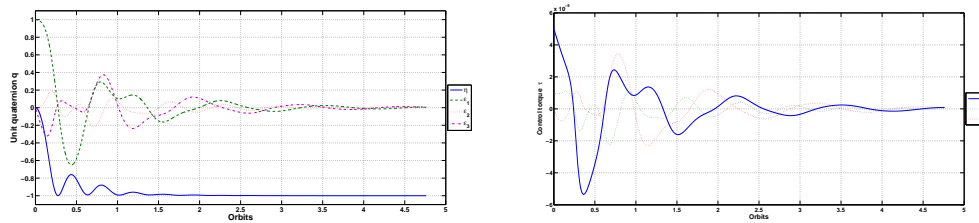


Figure 3. (Right) Time evolution of the control torque τ . (Left) Attitude error for $q_d = [-1 \ 0 \ 0 \ 0]^T$.

the controller of Remark 1. Second, we are not considering environmental disturbances like aerodynamic drag and solar radiation. Finally, as this work is part of a study of possible actuator/controller configurations it is necessary to consider other kinds of actuators, for instance, magnetic coils.

Referencias

1. CubeSat project webpage: <http://cubesat.atl.calpoly.edu>
2. Pisacante V. L.: **Fundamentals of Space Systems**, Oxford University Press, New York, 2005.
3. Nicklasson, P. J. and Kristiansen, R.: Satellite Attitude Control by Quaternion-Based Backstepping, *Procc. of the American Control Conference*, Portland, Oregon, June 8-10, 2005.
4. Sira-Ramírez, H.: Spacecraft Reorientation Maneuvers Via Linearizing Variable Structure Control, *20th Annual Asilomar Conference on Signals, Systems and Computers*, pp. 21-44, 1986.
5. Sira-Ramírez, H. : Are non-linear controllers really necessary in power electronics devices?, *European Power Electronics Conference EPE-2005*, Dresden, Germany, 2005.
6. Velasco-Villa, M., Rodríguez-Cortés H., Sanchez-Estrada, I. and Sira-Ramírez H. : Passivity based Path Tracking Control of an Omnidirectional Mobile Robot, submitted to *International Conference on Robotics and Automation* 2009.
7. Egeland, O. and Godhavn J. M., Passivity-based Adaptive Attitude Control of a Rigid Spacecraft, *IEEE Transactions on Automatic Control*, Vol. 39, No. 4, pp. 842-846, 1994.
8. Tsiotras, P.: Further Passivity Results for the Attitude Control Problem, *IEEE Transactions on Automatic Control*, Vol. 43, No. 11, pp. 1597-1600, 1998.
9. Wen J. T. and Kreutz-Delgado K.: The Attitude Control Problem, *IEEE Transactions on Aerospace and Electronic Systems*, Vol. 36, NO. 10, pp. 1148-1162, 1991.
10. DeVon, D. A., Fuentes R. J. and Fausz, J. L.: Passivity-Based Attitude Control for an Integrated Power and Attitude Control System using Variable Speed Control Moment Gyroscopes, *Procc. of the American Control Conference*, Boston, Massachusetts, June30- July 2, 2004.